NASA TECHNICAL MEMORANDUM

NASA TM X-62,357

PIONEER 10 OBSERVATIONS OF THE SOLAR WIND INTERACTION WITH JUPITER

J. H. Wolfe, J. D. Mihalov, H. R. Collard, and D. D. McKibbin
Ames Research Center
Moffett Field, Calif. 94035

L. A. Frank
Department of Astronomy and Physics
University of Iowa, Iowa City, Indiana

and

D. S. Intriligator
Physics Department University of Southern
California, Los Angeles, California

May 1974

PIONEER 10 OBSERVATIONS OF THE SOLAR WIND INTERACTION WITH JUPITER

J.H. Wolfe, J.D. Mihalov, H.R. Collard and D.D. McKibbin
Space Physics Branch, NASA Ames Research Center
Moffett Field, California 94035

L.A. Frank
Department of Physics and Astronomy, University of Iowa
Iowa City, Iowa 52240

D.S. Intriligator
Physics Department, University of Southern California
Los Angeles, California 90007

ABSTRACT

Detailed analysis of the Pioneer 10 Plasma Analyzer experiment flight data during the Jupiter flyby in late November - early December, 1973, has been performed. The observations show that the interaction of Jupiter's magnetic field with the solar wind is similar in many ways to that at earth, but the scale size is over 100 times larger. Jupiter is found to have a detached standing bow shock wave of high Alfvén Mach number. Like the earth, Jupiter has a prominent magnetopause which deflects the magnetosheath plasma and excludes its direct entry into the Jovian magnetosphere. Unlike the earth, the sunward hemisphere of Jupiter's outer magnetosphere is found to be highly inflated with thermal plasma and a high beta region which is highly responsive to changes in solar wind dynamic pressure. Observational arguments are presented which tend to discount a thin disk-like magnetosphere but, rather, favor a Jovian magnetosphere, albeit probably considerably flattened as compared to the earth's magnetosphere, yet still with reasonable thickness. Results concerning the shock jump conditions, the magnetosheath flow field and inferred internal magnetospheric plasma are presented.

1. THE PIONEER 10 MISSION

The Pioneer 10 spacecraft was successfully launched from Cape Kennedy on March 3, 1972 aboard an Atlas-Centaur launch vehicle which incorporated a TE-364-4 solid propellant third stage. At the time, Pioneer 10 attained the highest injection energy ever achieved as attested to by the fact that the spacecraft only required eleven hours to cross the lunar orbit. After a 21 month flight, the Pioneer 10 spacecraft arrived at its radius of closest approach (RCA) at Jupiter at a distance of approximately 2.8 R_J (Jovicentric Jupiter radii) on December 4, 1973.

The principal scientific objectives of Pioneer 10 are to investigate the nature of the interplanetary medium beyond the orbit of Mars, including the asteroid belt, and to make direct, in situ, observations of the planet Jupiter and its environment. The successful flyby of Jupiter by Pioneer 10 achieved the latter objectives, however, the interplanetary objectives are still being pursued in the present post-encounter mission beyond Jupiter. Present estimates are that the Pioneer 10 spacecraft can be utilized for interplanetary observations to a solar radial distance of at least 20 AU.

The Pioneer 10 spacecraft and trajectory details have been reported by Hall [1974] and are only briefly summarized here. The Pioneer 10 spacecraft weighs 258 kg including 33 kg for the 11 on-board experiments. Two additional experiments are performed using the spacecraft S-band communications system. The spacecraft is spin stabilized with a spin rate of 4.8 rpm. The spacecraft spin axis is parallel to the axis of the 2.74 m diameter high gain antenna reflector and is kept pointed toward the earth in order to maximize the communication bit rate. The maximum bit

rate used during the Jupiter encounter was 1024 bits per second. Spacecraft spin axis precession maneuvers are required periodically in order to maintain earth pointing and were performed approximately six days prior to and two days after the Jupiter flyby. During the encounter, the earth pointing spacecraft spin axis was oriented at an angle of approximately 9.2° with respect to the spacecraft-sun line in a direction away from the west limb of the sun. Electrical power for the experiments and spacecraft subsystems is supplied by four radioisotope thermoelectric generators (RTG) since a conventional solar cell array is not practical for the large solar distances involved in the Pioneer 10 mission. The RTGs are located approximately 2.4 m from the center of the spacecraft at the end of two long booms. Inspection of in-flight data indicates that these RTGs have produced negligible interference with any of the Pioneer 10 experiments. During the encounter the spacecraft approached Jupiter in the mid-morning sector of the sunlit hemisphere and exited near Jupiter's dawn meridian. For details of the flyby trajectory, see Hall [1974].

2. THE PLASMA ANALYZER INSTRUMENTATION

The Ames Research Center Plasma Analyzer experiment on Pioneer 10 consists of dual, 90°, quadrispherical electrostatic analyzers, multiple charged particle detectors and attendant electronics. This analyzer system is capable of determining the incident plasma distribution parameters over the energy range for protons from 100 to 18,000 ev and from approximately 1 to 500 ev for electrons. A central, cross sectional drawing of the analyzer and detector portions of the experiment is shown in Figure 1. The "A" detector or high resolution quadrispherical analyzer

(the inner analyzer system shown in Figure 1) has an analyzer constant of 9 (charged particle acceptance energy per unit charge divided by the analyzer plate potential) with an analyzer plate mean radius of 9 cm and 0.5 cm separation. The high resolution analyzer is used for ion analysis only and utilizes 26 Bendix type CEM 4012 Channeltrons, operated in the pulse counting mode, for ion detection. The Channeltron detectors are arranged in a semicircle at the base of the analyzer plates and cover the angular range of ± 51° with respect to the entrance aperture normal. The Channeltrons have an angular separation of approximately 3° near the central portion of the analyzer and approximately 8° separation at the extremes of the analyzer. The Channeltron bias voltage can be changed in two sections (left and right halves) by ground command in eight discrete steps over the range from 2600 to 4400 volts. Analysis of flight data has shown that all 26 Channeltrons have operated flawlessly since launch and no appreciable degradation has been observed prior to, during or subsequent to the Jupiter encounter.

The "B" detector or medium resolution analyzer (the outer analyzer system in Figure 1) has a 12 cm mean radius and 1 cm plate separation giving an analyzer constant of 6. The medium resolution analyzer is used for both ion and electron detection and utilizes five, flat surface, current collectors and electrometer amplifiers. The central three current collectors each have a 15° view width and cover an angular view range of ± 22.5° with respect to the entrance aperture normal. The two outside collectors each have an angular width of 47.5° and are located at ± 46.25° with respect to the center of the analyzer.

The Plasma Analyzer experiment is situated on the Pioneer 10 space-

craft such that the entrance apertures view back toward the earth (and therefore, the sun) through a wide slit in the back of the spacecraft high gain antenna reflector. The entrance aperture normals are oriented parallel to the spacecraft spin axis thus allowing a complete angular scan of the earthward hemisphere every half spacecraft revolution. The edges of the antenna reflector limit instrument viewing to ± 73° with respect to the spacecraft spin axis. Although there are a variety of possible operating modes for the experiment, the principal mode utilized during the encounter phase of the Pioneer 10 mission is one in which the energy per unit charge acceptance analyzer potential is stepped every one-half revolution of the spacecraft and all current collectors and Channeltrons are read out at the peak flux roll angle of the spacecraft. Since the medium and high resolution analyzers operate independently, a complete cross check between the two analyzers is possible. The combined analyzer system covers the dynamic range for charged particle fluxes from approximately 1×10^2 to 3×10^9 cm^{-2} sec^{-1} and is capable of resolving proton temperatures down to at least 2×10^3 °K. Both analyzers were calibrated prior to launch in the Ames Research Center Plasma Ion Calibration Facility. These pre-launch calibrations are utilized in a least-squares fit to the flight data for a variety of possible distribution models in order to determine the plasma ion distribution parameters. Whereas the preliminary report of the Ames Research Center Plasma Analyzer observations for the Pioneer 10 Jupiter encounter [Wolfe et al. 1974] was based on real time data, the results presented here are based on the analysis of the off-line flight data tapes. An isotropic Maxwellian distribution model has been assumed in the fit to the flight data reported here.

3. THE SOLAR WIND-JUPITER INTERACTION

The first unambiguous indication of the interaction of the solar wind with the Jovian magnetic field occurred on November 26, 1973, at approximately 1946 UT spacecraft time. The telemetry signals were actually received at about 2031 UT on earth (ground received time or GRT) corresponding to a one-way radio propagation time of approximately 45 minutes. Note that unless specifically indicated as GRT, spacecraft time will be used throughout this report. At this time the Pioneer 10 spacecraft was inbound toward Jupiter at a Jovicentric radial distance of 108.9 R_J (R_J = 71372 km). The two solar wind ion spectra shown in Figure 2 were taken in the interplanetary medium (spectrum on the left) at 1905 UT, GRT, on November 26, 1973 (Day 330) about 1 hour and twenty-five minutes before the Jovian bow shock crossing and in the Jovian magnetosheath (spectrum on the right) at 0451 UT, GRT, on November 27, 1973 (Day 331) about 8 hours and twenty minutes after the shock crossing. Although the ion characteristics in the magnetosheath were quite variable, the spectrum shown in Figure 2 is considered to be typical. The ragged appearance of this spectrum is most likely due to fluctuations in the magnetosheath ion characteristics during the period required to obtain the spectrum and are therefore considered to be an artifact in the data caused by sample aliasing. The observation of this drastic change in the ion spectral characteristics, illustrated in Figure 2, is interpreted as the encounter of the Pioneer 10 spacecraft with a detached bow shock wave standing off from Jupiter's magnetosphere and in many respects is quite similar to the case at earth.

For the interplanetary ion spectrum shown in Figure 2, the proton peak is seen near 1 kev and the doubly charged helium peak near 2 kev.

This interplanetary spectrum corresponds to a solar wind convective speed of approximately 440 km sec^{-1}, a proton number density of 0.05 cm^{-3} and an isotropic proton temperature of 5.4×10^3 °K. It should be noted that this solar wind speed and number density corresponds to an anomalously low solar wind dynamic pressure (by about a factor of 4) compared to that normally observed by this experiment in the interplanetary medium near 5 AU. The ion distribution parameters for the magnetosheath spectrum of Figure 2 can only be estimated due to the large angle (> approximately 50°) in the magnetosheath plasma flow direction with respect to the spacecraft spin axis which is 9.2° W with respect to the spacecraft-sun line. This large deflection in flow direction from approximately antisunward to a large angle with respect to the spin axis was observed as the spacecraft crossed the bow shock and, with the exception of a 45 minute period commencing at approximately 0815 UT on November 27, 1973, persisted throughout the entire magnetosheath traversal. During this 45 minute period the flow directions were within the sensitive look angle of the Plasma Analyzer and gave average magnetosheath plasma distribution parameters of 273 km sec^{-1} bulk speed, a proton number density of 0.62 cm^{-3} and a proton temperature of 3.5×10^5 °K. The distribution parameters for the magnetosheath spectrum of Figure 2 are similar: $v = 239$ km sec^{-1}; $T \gtrsim 1.2 \times 10^5$ °K. The magnetosheath flow field characteristics are discussed in more detail in the next section.

At 1953 UT on November 27, 1973, the incident plasma ion flux abruptly dropped below the sensitivity threshold for both the high and medium resolution analyzers. At this time the Pioneer 10 spacecraft was located at a Jovicentric radial distance of 96.4 R_J. This termination of the mag-

netosheath plasma flow is interpreted as the crossing of the magnetopause boundary and penetration into Jupiter's magnetosphere by Pioneer 10 and is presumed to be due to the exclusion and deflection of the magnetosheath plasma by the equal and opposite pressure exerted by Jupiter's outer magnetic field and its internal gas. As was the case for the bow shock, Jupiter's magnetopause also seems in many ways similar to earth's.

As the spacecraft proceeded inbound, magnetosheath plasma, flowing at large angles with respect to the spacecraft spin axis, was again observed at 0233 UT on December 1, 1973, corresponding to a radial distance of 54.3 R_J. The observation of magnetosheath plasma persisted for approximately eleven hours and was again abruptly terminated at 1336 UT on December 1, 1973, at 46.5 R_J. At present there are two apparent explanations for the second magnetopause traversal observed during the inbound portion of the Pioneer 10 trajectory. The first would be that the interplanetary solar wind dynamic pressure increased to such an extent that the entire Jovian magnetosphere contracted down to a size such that the spacecraft was again located in the magnetosheath. An alternative possibility is that the topology of Jupiter's magnetosphere is such that a simple change in the interplanetary solar wind flow direction (with little or no change in dynamic pressure) deflected Jupiter's magnetosphere so that the spacecraft was located within the magnetosheath. The present evidence seems to strongly favor the former explanation and is discussed further in the summary section.

During the remainder of the Pioneer 10 traversal of the Jovian magnetosphere, sporadic plasma ion fluxes were observed but their analysis has been complicated by high background rates due to penetrating energetic

electrons and protons. Magnetospheric plasma ion observations are very preliminary at this time and are not reported here. Other than these high background rates observed in Jupiter's inner magnetosphere, the Plasma Analyzer experiment successfully withstood Jupiter's intense radiation zones and recrossed Jupiter's magnetopause on the outbound leg of the trajectory at 1153 UT on December 10, 1973 at a distance of 97.9 R_J. In contrast to the inbound portion of the flyby trajectory, where the bow shock was observed once and the magnetopause was crossed three times, during the outbound leg the magnetopause was crossed five times and there were seventeen positively identifiable shock crossings. All of the shock and magnetopause observations during the Pioneer 10 Jupiter flyby are listed in Table 1 for both the inbound and outbound passes. In this table under spacecraft location, IP refers to interplanetary medium, MSH the Jovian magnetosheath and MS to Jupiter's magnetosphere. For each boundary observed (S for shock and M for magnetopause) the date and spacecraft time in UT and Jovicentric distance in R_J are listed. From Table 1 it is seen that the last shock crossing occurred at 1928 UT on December 22, 1973 at a distance of 242.6 R_J. Thus the Jupiter encounter for the Plasma Analyzer experiment lasted nearly a month!

Two further plasma observations associated with Jupiter's bow shock may be noted. A period of approximately 14 minutes duration, that began 13 hours and 43 minutes after the last bow shock crossing listed on Table 1, exhibits greatly reduced plasma flux and some flow deflection that probably indicates a movement of Jupiter's bow shock near the spacecraft. However, a crossing of the bow shock can not be positively identified here. In addition, 18 minutes before the first bow shock crossing the solar wind

plasma flux was apparently temporarily greatly reduced which could be an interplanetary effect rather than an approach of the bow shock near the spacecraft since a large flow deflection was not observed.

The magnetosheath boundary traversals given in Table 1 are illustrated in Figure 3, which shows the Pioneer 10 Jupiter encounter trajectory projected onto Jupiter's orbital plane. Each shock (S) and magnetopause (M) location is identified along the spacecraft trajectory at the position where it was observed. Note that in the outbound leg, the point identifying the second magnetopause location actually represents two closely spaced magnetopause crossings and a burst of plasma which could represent two further crossings, and the point identifying the last shock observation represents five separate crossings (see Table 1). The dashed lines in Figure 3 are for illustrative purposes only and are meant to show the extremes in magnetopause and shock locations during the Pioneer 10 flyby. The boundary shapes and shock standoff distances have been determined from the gas dynamic analog [Spreiter et al., 1966]. The shock and magnetopause boundaries have been arbitrarily made symmetrical with respect to the Jupiter-solar wind line. The outermost shock and magnetopause boundaries have been scaled to the last shock crossing for the outbound leg. Similarly the innermost shock and magnetopause boundaries have been scaled to the last magnetopause crossing for the inbound leg.

It is interesting to consider the large scale size of Jupiter's magnetosphere and shock front. For example, the width of the shock front for its largest extent (based on the last shock crossing on the outbound leg and assumed symmetry and shape illustrated in Figure 3) would correspond to a distance of approximately 485 R_J as measured across the dawn-dusk

meridian. This is equivalent to a width of 0.23 AU and is more than 2 orders of magnitude larger than the nominal width of the earth's bow shock. The large extent over which Jupiter's magnetosphere can evidently move indicates that it is extremely responsive to changes in the incident solar wind conditions.

4. THE MAGNETOSHEATH FLOW FIELD

Figure 4 gives half-hour averages of proton bulk velocities, number densities and lower limit isotropic temperatures observed during November 26 and 27, 1973 as Pioneer 10 first crossed Jupiter's bow shock and magnetosheath. The velocities presented do not have the spacecraft velocity subtracted. A correction for this may be estimated by use of the spacecraft velocity components during this two day period, which are 7.2 to 7.5 km sec^{-1} in the antisolar direction, and 6.7 ± 0.1 km sec^{-1} in the direction of planetary motion, parallel to the ecliptic plane.

The bow shock and magnetopause locations as observed by the Plasma Analyzer are indicated with a solid and an open arrow, respectively, at the bottom of Figure 4. Within the inbound magnetosheath, plasma parameters could not be determined by the medium resolution detector due to deflection of the peak plasma flow outside of its angular acceptance range, except during 0815 to 0900 on November 27. For this time period proton velocities and temperatures from the medium resolution detector were determined by a fit of a Maxwellian distribution to the data. The average proton number density obtained is 0.56 cm^{-3}. For all magnetosheath times on the figure, half-hour averages of proton bulk velocities and lower limit temperatures from the high resolution detector are given.

The plasma parameters from the medium resolution detector given here

are calculated by a linear least-squares fit of the flight data to a convecting isotropic temperature Maxwell-Boltzmann distribution, using a representation of the detector response condensed from detailed laboratory calibration data.

The velocities and temperatures from the high resolution detector data are obtained following the formalism of a calculation of the moments of the plasma velocity distribution. The proton counts from one of the outermost Channeltrons of the high resolution detector are used. These are integrated, except during special instrument modes, for 31/64 of a spacecraft revolution for successive energy acceptance values of the analyzer plate voltages during this time. These count values are treated as samples of the proton velocity distribution that are equally weighted in velocity space. Then the bulk velocity is obtained from

$$N < \vec{p} > = m\, N\, (\langle \vec{V} \rangle - \vec{u}) = 0$$

and this condition is approximated by

$$u \sim \frac{\Sigma\, n_i\, v_i}{\Sigma\, n_i} \quad .$$

This gives the velocity value u such that the momentum density of the protons is zero in a frame moving with this velocity. Here n_i is the count value for the i^{th} velocity (energy) analyzer acceptance value v_i, m is the proton mass, N the proton volume density, $\langle \vec{p} \rangle$ the vector average proton momentum and $\langle \vec{V} \rangle - \vec{u}$ the vector average proton velocity (thermal velocity) referred to the proton bulk velocity u. Similarly the lower limit temperature value is obtained from

$$T = \frac{m}{3k}\left[\Sigma\, n_i\, (u - v_i)^2\right] / \Sigma\, n_i$$

where k is Boltzmann's constant.

When these calculations are performed, an attempt is made to eliminate detector responses due to He^{++} by not using the portion of the spectrum for E/q (energy per unit charge) values two times or greater than that for the peak counts. This is one reason why the magnetosheath temperatures from the high resolution detector are lower limits, since the interplanetary spectra just upstream from the shock indicate a negligibly low He^{++} solar wind abundance at that time (see Figure 2). If the high resolution detector temperature calculation described above is repeated anywhere during this first inbound magnetosheath traversal using the entire spectrum observed, as if the He^{++} contribution were negligible, the calculated temperatures nearly all exceed 10^6 °K, while the magnetosheath values reported in Figure 4 are in the $\sim 2 \times 10^5$ °K range. The magnetosheath temperatures reported here are also lower limits since the angular scan of the proton velocity distribution by the outermost Channeltrons used here is not expected to include the peak of the distribution except coincidentally. The peak of the distribution is believed to move both inside and outside the scan of the outermost Channeltrons ($\sim 50°$ with respect to the spacecraft spin axis) during this time, as is readily seen in the data but not presented here. This motion of the peak could bias the velocities reported, as well as the temperatures. Also, the roll-integration of the outermost Channeltron count rates introduces an effect that could broaden the velocity distributions used in the temperature calculation, but this effect is believed to be negligible. The medium resolution detector magnetosheath temperatures given on Figure 4 agree with the lower limit high resolution detector temperatures, presumably because the medium resolution detector data have been fit to an isotropic Maxwellian distribution so that the

non-Maxwellian portions of the spectrum are ignored. This tends, in this case, to reduce the magnetosheath temperature calculated from the medium resolution detector data.

The medium resolution detector magnetosheath proton bulk velocities determined for the 45 minute period beginning at 0815 on November 27, 1973, were generally 50 km sec^{-1} lower than the high resolution detector values. The proton velocity distribution had, however, a high-energy non-Maxwellian tail at that time which is accounted for in the high resolution detector velocity calculation, but which tends to be ignored when the medium resolution detector data are fit to a Maxwellian. Bulk velocities calculated from an unweighted least squares fit of a parabola to the velocity distribution reported by the high resolution detector, including the effects of thermal speeds, agree closely with the medium resolution detector magnetosheath velocities for this 45 minute period. Unweighted fits to a parabola are used because weighted fits reduce the statistical weight of the low velocity points in these measured magnetosheath velocity distributions to the extent that they are often ignored with the result that a meaningful velocity determination is then not obtained.

Gaps in the data of Figure 4 are sometimes due to ground-commanded changes of instrument status into special modes for which plasma parameter calculation techniques were not completed in time for the results to be included here. Some gaps are also caused by brief data losses in the ground data network and, in the case of the magnetosheath data, occasionally to an observed spectrum without one prominent maximum so that an estimate of the He^{++} portion of the spectrum to be ignored could not readily be made.

The second inbound magnetosheath traversal (not plotted here) on

December 1 between 54.3 and 46.5 R_J is characterized by somewhat lower proton bulk velocities than the first magnetosheath traversal shown in Figure 4. The average velocity calculated by the moment method described above is 246 km sec^{-1} from 0234 to 1313 UT on December 1 during the second magnetosheath traversal, but it is 273 km sec^{-1} at 1950 UT, November 26 to 1937 UT, November 27 during the first traversal.

Except for the initial sample, the second magnetosheath traversal proton bulk velocities start near 190 km sec^{-1} at $\sim$ 0245 UT, December 1, and tend to gradually rise to $\sim$ 280 km sec^{-1} values at 1245 UT. The unaberrated polar and azimuthal flow directions at the beginning of the traversal are $\gtrsim$ 40 deg southward and $\sim$ 19 deg in the direction of planetary motion, respectively. Near $\sim$ 0715 UT, there are several samples with lower limit southward flow directions near zero degrees, and azimuthal flow directions $\sim$ 35 deg in the direction of planetary motion (direction opposite normal aberration). Near the end of the traversal the flow direction is $\sim$ 15-25 deg southward and $\sim$ 30-35 deg in the direction of planetary motion.

The proton temperatures appear somewhat higher during the second traversal, compared to the first, by perhaps as much as a factor of two and the observed densities were comparable.

Figure 5 gives half-hour averages of proton bulk velocities, number densities, isotropic temperatures and hourly averages of unaberrated azimuthal and polar angles for the outbound traversal of Jupiter's magnetosheath by Pioneer 10, during December 10 through 22, 1973. The flow direction average polar, $\bar{\theta}$, and azimuthal, $\bar{\varphi}$, angles are composed from individual samples θ_i and φ_i using the expressions

$$\sin \bar{\theta} = \frac{\Sigma \sin \theta_i}{\left[\left(\Sigma \cos \theta_i \cos \varphi_i \right)^2 + \left(\Sigma \cos \theta_i \sin \varphi_i \right)^2 + \left(\Sigma \sin \theta_i \right)^2 \right]^{\frac{1}{2}}}$$

and $\tan \bar{\varphi} = \left[\Sigma \cos \theta_i \sin \varphi_i \right] / \left[\Sigma \cos \theta_i \cos \varphi_i \right]$. Polar angles, θ, are positive for southward flow, while azimuthal angles, φ, are positive for solar wind flow deviated in the direction opposite planetary motion. The velocity averages given on this figure have not had the spacecraft velocity subtracted. The correction for this may be estimated using the spacecraft velocity components which are 0.4 and 23.7 km sec^{-1} in the antisolar direction and the direction of planetary motion (but parallel to the ecliptic), respectively, at 1200 UT on December 10. These velocity components are 0.7 and 22.7 km sec^{-1}, respectively, at 0000 UT on December 22. The times of seventeen bow shock and five magnetosheath crossings, listed in Table 1, are shown on Figure 5 and indicated by hollow and solid arrows, respectively, at the bottom of the figure.

Gaps in the plots of parameters on Figure 5 are sometimes due to ground-commanded changes into experiment modes for which plasma parameter calculations are not available for inclusion in this paper. In addition, at some times, in the magnetosheath, the medium resolution detector currents are reduced to the instrument noise levels, while the high resolution detector data have not been analyzed for this time period. During the times on this figure within the magnetosphere, proton fluxes are not detectable in the data with the standard techniques used for the other portions of the figure.

Inspection of Figure 5 shows large bulk velocity excursions for Dec.10 and early on Dec.11. Part of the cause of this may be thought of as response of the Maxwellian model, in the computer routine which cal-

culates the plasma parameters, to an apparent non-Maxwellian plasma spectrum with a very broad proton maximum. At various times the computer program weights the higher velocity portion of this broad maximum more or less heavily, and thus calculates higher or lower proton bulk velocities.

The magnetopause crossings from 0943 to 0958 UT on December 12 have the characteristic of relatively gradual disappearance or reappearance of all observable plasma flux as the magnetosphere is entered or left behind.

Perhaps the most striking features in Figure 5 are the much less dramatic changes in velocity and density for the shock crossings further away from the planet as compared to the inbound shock crossing or closer crossings for the outbound leg. Note, however, that relatively large changes in the proton temperature are always observed regardless of shock location. As is the case at earth, this probably indicates that Jupiter's bow shock becomes weaker for greater and greater angles and distances from the subsolar point. For this reason, the determinations of the shock locations reported here have relied more heavily on the temperature changes rather than on any other parameter, although the flow direction changes are usually very prominent in the high resolution detector data.

In addition, as was the case for the inbound magnetosheath traversals, the flow directions in the magnetosheath seen in Figure 5 are greatly deviated, in general agreement with those expected for plasma flow around a relatively blunt magnetosphere. A large southward component in the magnetosheath flow was observed for the inbound leg when the spacecraft was below Jupiter's orbital plane. Here a large northward component in the flow is seen where for the outbound magnetosheath traversal the space-

craft is above Jupiter's orbital plane.

5. SHOCK JUMP CONDITIONS

Table 2 gives the measured average and calculated best estimate shock jump parameters and "sigma noise parameters" for the inbound Jupiter bow shock crossing observed by Pioneer 10. The best estimate values are calculated by use of the Lepping and Argentiero [1970] program, without an error cone calculation. The vector components in the table are given in the standard right-handed ecliptic-type coordinate system with positive x in the solar direction and positive z northward. The subscripts 1 and 2 refer to upstream and downstream parameters, respectively. B and n are respectively the magnetic field (E. J. Smith, private communication) and the proton number density. W is the difference between downstream and upstream bulk velocity components. Eight upstream and seven downstream magnetic field one-minute averages were used, as well as three upstream and three downstream proton bulk velocity samples and three upstream proton number density samples. The basic upstream plasma sampling period is 5.4 minutes. The downstream proton number density best estimate value is that which produces the best fit when a variety of assumed values are entered into the program as input observed data. The downstream number densities immediately adjacent to the shock are difficult to measure accurately because of the apparent proximity of the flow direction to the outer edges of the detector acceptance.

The measured and calculated best estimate parameters agree well except for the x component of the downstream magnetic field and the z component of the downstream and upstream velocity difference. With regard to the downstream x component of the magnetic field, the measured values

closest to the shock transition are higher and so are closer to, although still lower than, the calculated best-estimate value. The z component of the velocity downstream from the shock is difficult to estimate from the data, again because of the proximity of the plasma flow direction to the edge of the instrument acceptance. There does seem to be a consistent trend in the data, just downstream from the shock, toward average observed W_z values at least as large in magnitude as that given on Table 2.

The calculated best-fit shock normal is (.841, -.056, -.538), indicating only a 4 deg angle between the solar direction and the projection of the shock normal on the plane that contains both the solar direction and the y axis of the coordinate system. A 33 deg southward tilt of the shock normal is also indicated. The pronounced and chiefly southward tilt of the bow shock indicated by this best-fit shock normal, as well as the apparent large and chiefly southward plasma flow deflection at the shock, both are suggestive of the solar wind interaction with a large blunt obstacle. The calculated best-fit pressure difference across the shock (downstream less upstream) is 4×10^{-11} dynes cm^{-2}. The measured pressure difference due to protons alone is at least 12×10^{-13} dynes cm^{-2}, assuming that the downstream proton number density is .15 cm^{-3}. The Alfvén Mach number of the shock, assuming it is stationary, is 10., using the best-fit shock orientation.

Table 3 gives measured average and calculated best estimate shock jump parameters, and "sigma noise parameters" for the third shock crossing observed by Pioneer 10 on the outbound leg. The same techniques are used as those employed for the inbound shock calculations. Seventeen upstream and ten downstream one-minute magnetic field averages (E. J. Smith, private

communication) were used. Two upstream and three downstream proton density measurements were used taken at 2.8 min intervals. Only one upstream and one downstream proton bulk velocity sample was used. The vector components in the table are given in the same coordinate system used for the inbound case. As before the subscripts 1 and 2 refer to upstream and downstream parameters, respectively, B and n are respectively the magnetic field and the proton number density and W_i are the differences between downstream and upstream bulk velocity components.

Here again there is good agreement between measured and best estimate parameters. The best fit calculated shock normal (outward) is (.379, -.887, .264), indicating a 67 deg angle between the solar direction and the projection of the normal on the plane that contains both the solar direction and the y axis of the coordinate system. This angle appears $\sim$ 15 deg larger than that expected for a shock shape like that of the earth. A 15 deg northward tilt of the normal is also indicated. The calculated best-fit thermal pressure difference across the shock is -2×10^{-11} dynes cm^{-2}. The measured pressure difference due to protons alone is 5×10^{-13} dynes cm^{-2}. The Alfvén Mach number of the shock for a shock stationary with respect to Jupiter is 8.5 using the best-fit orientation.

6. MAGNETOSPHERIC PLASMA

Table 4 gives estimates of magnetospheric plasma properties using two different methods. The first method assumes pressure balance across the magnetopause, expressed by

$$n_1 k (T_{e1} + T_{i1}) + \frac{B_1^2}{2\mu_0} = n_2 k (T_{e2} + T_{i2}) + \frac{B_2^2}{2\mu_0} .$$

The second method uses the aerodynamic analogy (cf. Spreiter et al. [1966]) and is described below. In the above pressure balance equation, the subscripts 1 and 2 refer to magnetosheath and magnetosphere parameters respectively, n is the plasma ion number density, T_e and T_i are the electron and ion temperatures, respectively, B is the magnetic field magnitude, k is Boltzmann's constant and μ_0, the magnetic permeability of free space, is $4\pi \times 10^{-7}$ Henrys m^{-1}. $T_e \sim T_i$ is assumed, and $T_{i2} \sim 5 \times 10^4$ °K ($\sim$ 4 ev electrons) is assumed based on the measured magnetospheric electron energy spectra [Intriligator and Wolfe 1974].

The magnetosheath values for the December 13 crossing are less reliable than the others due to divergence of the plasma flow direction near the outer limit of the medium resolution detector angular acceptance. The December 10 crossing appeared to occur at a time of extreme conditions and in addition the observed magnetic field profile across the magnetopause (E. J. Smith, private communication) appears as if a wide layer was crossed, but fields outside this "layer" are ignored when the results of the Table are calculated.

The results on Table 4 obtained with the aerodynamic analogy use Pioneer 10 free-stream plasma parameters obtained closest in time to the indicated magnetopause crossings. Because of the time delay between the magnetospheric and free-stream measurements by Pioneer 10 this method is less reliable due to neglect of possible time variations in the external free-stream conditions. The assumed condition is

$$K\, m\, n_1^*\, v^{*2} \cos^2\theta + n_1^*\, k\, (T_{e1}^* + T_{i1}^*) + \frac{B_1^{*2}}{2\mu_0} = n_2\, k\, (T_{e2} + T_{i2}) + \frac{B_2^2}{2\mu_0} \quad ,$$

where m is the proton mass, v the bulk velocity, the asterisks denote free-stream quantities, K is taken as unity and θ is the angle between the magnetopause normal and the free-stream plasma flow direction. θ is obtained from calculations made for the case at earth given by Spreiter et al. [1966]. The values of θ were tested against calculated values obtained using the magnetic field measured across the magnetopause (E. J. Smith, private communication) and assuming the magnetopause is a tangential discontinuity. The earth analogy values were much larger than the calculated values. This result implies a magnetopause body shape comparatively more blunt than the case of earth.

7. SUMMARY AND CONCLUSIONS

Of particular interest is the understanding of the topology and dynamics of Jupiter's magnetosphere and its interaction with the solar wind. This, of course, is difficult to do in a single flyby. There are, however, several clues in the Pioneer 10 data which shed some light on this problem. It is clear that in many respects Jupiter's standing bow shock, magnetosheath flow field and magnetopause are similar to the case at earth. Both the shock and magnetopause at Jupiter are observed to be well defined boundaries and like at earth, Jupiter's bow shock is a strong shock (high Alfvén Mach number). Jupiter's magnetopause, also like earth's, is a relatively sharp boundary between the planetary field and the magnetosheath flow field wherein it deflects the magnetosheath plasma and excludes it from direct entry into the magnetosphere. Finally, as is the case at earth, the observed shock normals and magnetosheath plasma flow directions observed for Jupiter are consistent with Jupiter's magnetosphere presenting a relatively blunt body to the solar

wind for the sunward hemisphere.

It is cautioned, however, that earth analogies may be confused due to the vastly different scale sizes involved. For example, the extent of Jupiter's bow shock, as inferred from the furthest out observed shock crossing, is almost a quarter of an AU wide as measured across the dawn-dusk meridian. This is over 2 orders of magnitude larger than the earth's bow shock measured in the same fashion. It is suspected that if Jupiter's magnetosphere were scaled down to the size of the earth's magnetosphere corresponding to the geocentric distance to the subsolar point, Jupiter's magnetosphere would be considerably flattened in shape as compared to the earth's. This is strongly suggested by the manner in which Jupiter's magnetic field lines in the outer magnetosphere are greatly elongated and stretched out from the planet [Smith et al., 1974a]. The degree to which Jupiter's magnetosphere is flattened is impossible to estimate from the data of this single flyby, but the plasma observations can at least place lower limits.

First of all, it is exceedingly unlikely that Jupiter's outer magnetosphere rotates rigidly and wobbles up and down coincident with the rotational period of Jupiter's tilted magnetic dipole (15° tilt reported by Smith et al. [1974a]) as suggested by Van Allen et al. [1974]. The inferred outer magnetosphere plasma densities are sufficiently high such that the measured magnetic field [Smith et al., 1974a] would not be able to contain the plasma much beyond about 20 R_J. The complicating factor seems to be the very narrow latitude extent over which energetic charged particles seem to be confined in Jupiter's outer magnetosphere [Fillius and McIlwain, 1974; Simpson et al., 1974; Trainor et al., 1974; Van Allen

et al., 1974]. A much more plausible model seems to be that suggested by Smith et al. [1974b], where a disturbance field associated with a current sheet is present in Jupiter's outer magnetosphere. This current sheet lies parallel to Jupiter's equatorial plane, contains the observed quasi-trapped energetic particle population, is the plane of symmetry for the flattened magnetosphere and moves up and down in latitude coincident with Jupiter's rotational period.

The question of the degree of flattening for Jupiter's outer magnetosphere still remains. During the inbound portion of the Pioneer 10 trajectory, the magnetopause was first observed at approximately 96 R_J and the spacecraft remained inside the magnetosphere for several days and, of course, many Jupiter rotational periods. Since the magnetosheath was not observed during this period, and since the Pioneer 10 spacecraft was 7 R_J below Jupiter's equatorial plane, then it follows that the thickness of Jupiter's magnetosphere must be at least four times this distance or 28 R_J. Likewise on the dawn side of Jupiter for the outbound pass, the spacecraft was within the magnetosphere for many Jupiter rotational periods prior to the last magnetopause crossing at approximately 150 R_J. In this region, Pioneer 10 was 24 R_J above Jupiter's equatorial plane, thus suggesting that here Jupiter's magnetosphere must be at least 96 R_J thick. These are probably conservative lower limits for the magnetospheric thickness, at least since fluctuations in the polar flow direction of the interplanetary solar wind would require the magnetosphere be thicker than the above values in order to avoid detection of the magnetosheath for time periods greater than one Jupiter rotation. Perhaps further

detailed analysis and correlation of plasma and magnetic field data could be used to increase these lower limits of the magnetospheric thickness.

One further argument against a disk-like magnetosphere and in favor of a magnetosphere with reasonable thickness, is the second inbound magnetosheath observation made near 50 R_J. If Jupiter's magnetosphere were a disk with the subsolar point near 100 R_J, then it can be argued that a simple shift in the solar wind polar flow direction could deflect the "magnetodisk" such that the Pioneer 10 spacecraft entered the magnetosheath. If this were true the spacecraft would find itself some 50 R_J downstream from the subsolar point and one would expect the magnetosheath plasma flow to be nearly solar radial. This in fact was not observed, but rather, the flow directions observed during the second magnetosheath traversal were incident from large angles with respect to the solar direction and quite similar to those observed during the first magnetosheath crossing. In addition, Jupiter's outer magnetosphere is apparently a high beta region with inferred thermal plasma densities on the order of a few cm^{-3}. This is supported by the outer magnetosphere magnetic field observations [Smith et al., 1974a] where hourly averaged field strengths are only slowly increasing from about 5-6 gamma at 100 R_J to slightly over 10 gamma at 30 R_J. This indicates that the entire outer portion of Jupiter's magnetosphere is highly inflated and therefore highly responsive to changes in the dynamic pressure of the solar wind.

A crude calculation shows that for the estimated internal pressure of Jupiter's outer magnetosphere, an increase in the solar wind dynamic pressure of only a factor of 3 is all that would be required to contract the magnetosphere from 100 R_J down to less than 50 R_J. At the time of

the Pioneer 10 encounter, Pioneer 11 was 2.2 AU upstream from Jupiter and almost aligned along the same solar radial (0.8 deg angular difference in solar longitude between Pioneer 11 and Jupiter). Approximately seven days seventeen hours prior to the second inbound magnetosheath traversal by Pioneer 10, a solar wind dynamic pressure increase of approximately 4 was observed by Pioneer 11. The delay time expected for this dynamic pressure increase to reach Jupiter is in excellent agreement with the entry of Pioneer 10 into Jupiter's magnetosheath for the second time during the inbound pass. Inspection of the hourly averaged magnetic field values for this second magnetosheath traversal [Smith et al., 1974a], shows a much higher field strength here as compared to the first traversal, indicating the magnetosheath field had been compressed. It is postulated, therefore, that Jupiter's magnetosphere contracted by at least a factor of 2 in response to an increase in the solar wind dynamic pressure, such that the Pioneer 10 spacecraft became imbedded in Jupiter's magnetosheath for the second time during the inbound leg.

The large number of magnetopause and shock crossings observed during the outbound pass further argues for the great responsiveness that Jupiter's outer magnetosphere must have to changing conditions in the solar wind. For this reason and the arguments in favor of a reasonably thick magnetosphere, the anomalously short distance observed across the first magnetosheath traversal is considered to be best accounted for by an outward expansion of Jupiter's magnetosphere at that time.

A fundamental question remaining concerns the point that if Jupiter's magnetosphere has a reasonable thickness, then why is the energetic particle population constrained to such a narrow disk in the outer magnetosphere?

Could the current sheet suggested by Smith et al. [1974b] form a sort of magnetic bottle or is there perhaps local acceleration [Simpson et al., 1974]? It is clear that deeper analysis will be required to shed further light on this question as well as observations on future Jupiter flybys (such as Pioneer 11) and orbiter missions.

ACKNOWLEDGMENTS

We are deeply indebted to Ed Smith for providing us with detailed magnetic field data prior to publication. This data has been essential for our shock and pressure balance calculations. We would like to express our appreciation and gratitude to the Pioneer Project Office at Ames Research Center for their hard work and excellent performance which produced the successful Pioneer 10 Jupiter flyby. We also thank the staff of TRW Systems, Redondo Beach, California, the Pioneer 10 spacecraft contractor, for the design and fabrication of the spacecraft which has operated flawlessly throughout the entire mission. Finally we would like to acknowledge the Management and Engineering Staff of Time Zero Laboratories, Torrance, California, for the detailed design and construction of the Pioneer 10 Plasma Analyzer experiment which has not only operated flawlessly since launch, but has exceeded operational expectations.

REFERENCES

Fillius, R.W. and C.E. McIlwain, Radiation Belts of Jupiter, Science, 183, 314, 1974.

Hall, C.F., Pioneer 10, Science, 183, 301, 1974.

Intriligator, D.S. and J.H. Wolfe, Initial Observations of Plasma Electrons from the Pioneer 10 Flyby of Jupiter, J. Geophys. Res., 79, , 1974.

Lepping, R.P. and P.D. Argentiero, Improved Shock Normals Obtained from Combined Magnetic Field and Plasma Data from a Single Spacecraft, Goddard Space Flight Center Report X-692-70-276, July, 1970 (see also J. Geophys. Res., 76, 4349, 1971).

Simpson, J.A., D. Hamilton, G. Lentz, R.B. McKibben, A. Mogro-Campero, M. Perkins, K.R. Pyle, A.J. Tuzzolino and J.J. O'Gallagher, Protons and Electrons in Jupiter's Magnetic Field: Results from the University of Chicago Experiment on Pioneer 10, Science, 183, 306, 1974.

Smith, E.J., L. Davis, Jr., D.E. Jones, D.S. Colburn, P.J. Coleman, Jr., P. Dyal and C.P. Sonett, Magnetic Field of Jupiter and Its Interaction with the Solar Wind, Science, 183, 305, 1974a.

Spreiter, J.R., A.L. Summers and A.Y. Alksne, Hydromagnetic Flow Around the Magnetosphere, Planet. Space Sci., 14, 223, 1966.

Trainor, J.H., B.J. Teegarden, D.E. Stilwell, F.B. McDonald, E.C. Roelof and W.R. Webber, Energetic Particle Population in the Jovian Magnetosphere: A Preliminary Note, Science, 183, 311, 1974.

Van Allen, J.A., D.N. Baker, B.A. Randall, M.F. Thomsen, D.D. Sentman and H.R. Flindt, Energetic Electrons in the Magnetosphere of Jupiter, Science, 183, 309, 1974.

Wolfe, J.H., H.R. Collard, J.D. Mihalov and D.S. Intriligator, Preliminary Pioneer 10 Encounter Results from the Ames Research Center Plasma Analyzer Experiment, Science, 183, 303, 1974.

(insert above)
Smith, E.J. et al., J. Geophys. Res., 79, , 1974b.

FIGURE CAPTIONS

Table 1 Jupiter Magnetosheath Boundary locations observed during the Pioneer 10 flyby. IP refers to the interplanetary medium, MSH is the magnetosheath, MS is the magnetosphere, S denotes a shock crossing and M a magnetopause crossing.

Table 2 The measured average and calculated best-estimate shock jump parameters and sigma noise parameters for the Pioneer 10 inbound Jupiter bow shock crossing.

Table 3 The measured average and calculated best-fit shock jump parameters and sigma noise parameters for the third shock crossing observed by Pioneer 10 for the outbound portion of the Jupiter flyby trajectory.

Table 4 The estimated Jupiter magnetospheric plasma properties assuming pressure balance across the Jovian magnetopause.

Figure 1 Central, cross sectional schematic of the analyzer and detector portions of the Pioneer 10 Ames Research Center Plasma Analyzer experiment.

Figure 2 Comparison of solar wind ion spectra taken upstream and downstream from Jupiter's bow shock for the inbound portion of the Pioneer 10 Jupiter flyby.

Figure 3 Locations of the shock (S) and magnetopause (M) crossings on the Pioneer 10 Jupiter flyby trajectory which has been projected onto Jupiter's orbital plane. The inner and outer

pair of dash lines illustrate the observed extremes of position of the magnetopause and standing bow shock. The shape of the boundaries and the shock stand-off distances are based on the gas dynamic analog and scaled to the actual boundary observations.

Figure 4 Half hour averages of the proton bulk velocities, number densities and lower limit isotropic temperatures observed for November 26 and 27, 1973 corresponding to the first crossing of Jupiter's bow shock and magnetosheath.

Figure 5 Half hour averages of the proton bulk velocities, number densities, isotropic temperatures and hourly averages of unaberrated azimuthal and polar angles for the outbound traversal of Jupiter's magnetosheath by Pioneer 10 during December 10 through 22, 1973.

TABLE 1
MAGNETOSHEATH BOUNDARIES

SPACECRAFT LOCATION	BOUNDARY OBSERVATION	SPACECRAFT TIME '73 DATE	SPACECRAFT TIME UT	DISTANCE R_J
		INBOUND		
IP	S	26 Nov	1946 ±2	108.90
MSH	M	27 Nov	1953 ±2	96.36
MS	M	1 Dec	0233 ±6	54.32
MSH	M	1 Dec	1335.7 ±2.2	46.50
MS				
		OUTBOUND		
MS	M	10 Dec	1153.4 ±0.5	97.92
MSH	M	12 Dec	0943.2 ±0.5	121.52
MS	M	12 Dec	0958.2 ±0.5	121.66
MSH	S	12 Dec	1453.2 ±1.5	124.14
IP	S	12 Dec	1950.7 ±6	126.64
MSH	M	13 Dec	0158.1 ±0.5	129.73
MS	M	14 Dec	1850 ±1	150.08
MSH	S	18 Dec	0328 ±1	188.87
IP	S	20 Dec	2145.1 ±0.5	220.54
MSH	S	20 Dec	2233.9 ±0.5	221.41
IP	S	21 Dec	0212 ±2	223.13
MSH	S	21 Dec	0643 ±2	225.27
IP	S	21 Dec	1027 ±2.8	227.04
MSH	S	21 Dec	1158 ±2	227.76
IP	S	21 Dec	1848.5 ±9.5	230.99
MSH	S	21 Dec	1929.2 ±2.9	231.31
IP	S	22 Dec	0605 ±10	236.31
MSH	S	22 Dec	1757.6 ±1.8	241.44

IP				
	S	22 Dec	1805 ±1	241.97
MSH				
	S	22 Dec	1811.8 ±1.5	242.02
IP				
	S	22 Dec	1815.7 ±0.1	242.05
MSH				
	S	22 Dec	1928.0 ±2.7	242.62
IP				

Note: MS plasma bursts at 0225 and 1345, December 1, and 0947.7, December 12. Greatly reduced MSH plasma flux at 1324.8 ± 0.5, December 1.

Table 2

Parameter	Average value	σ	Best estimate value
B_{1x} (gamma)	-.46	.14	-.36
B_{1y}	.11	.24	.11
B_{1z}	-.01	.21	.08
B_{2x}	-.18	.32	-.61
B_{2y}	.38	.53	.46
B_{2z}	-.47	.30	-.35
W_x (km sec^{-1})	197.	35.	208.
W_y	-5.	15.	-9.
W_z	-316.	85.	-142.
n_1 (cm^{-3})	.042	.01	.034
n_2	---	---	.15

Table 3

Parameter	Average value	σ	Best estimate value
B_{1x}(gamma)	.02	.30	.00
B_{1y}	-.94	.29	-.95
B_{1z}	.27	.16	.28
B_{2x}	-2.11	1.06	-1.88
B_{2y}	-1.84	1.02	-1.70
B_{2z}	.48	.58	.46
W_x(km sec^{-1})	55.	20.	78.
W_y	-9.0	20.	.8
W_z	4.8	15.	1.2
n_1 (cm^{-3})	.21	.1	.18
n_2	.24	.15	.32

Table 4

	Magnetosheath		Magnetosphere			
Time (UT)	Thermal Pressure ($dynes\ cm^{-2}$)	Magnetic Energy Density ($erg\ cm^{-3}$)	Calculated Thermal Pressure ($dynes\ cm^{-2}$)	Calculated Beta	Calculated Ion Number Density (cm^{-3})	Magnetic Energy Density ($erg\ cm^{-3}$)
Dec 10-1153	12×10^{-11}	44×10^{-11}	12×10^{-11}	0.28	8.4	44×10^{-11}
Dec 13-0158	0.4×10^{-11}*	2.9×10^{-11}	0.4×10^{-11}	0.13 ~0.2+	0.27 0.43+	2.9×10^{-11}
Dec 14-1850	7.1×10^{-11}	4.1×10^{-11}	7.6×10^{-11}	2.1 ~2.8+	5.5 7.3+	3.6×10^{-11}

*measured value not too reliable.
+estimated using aerodynamic analogy.

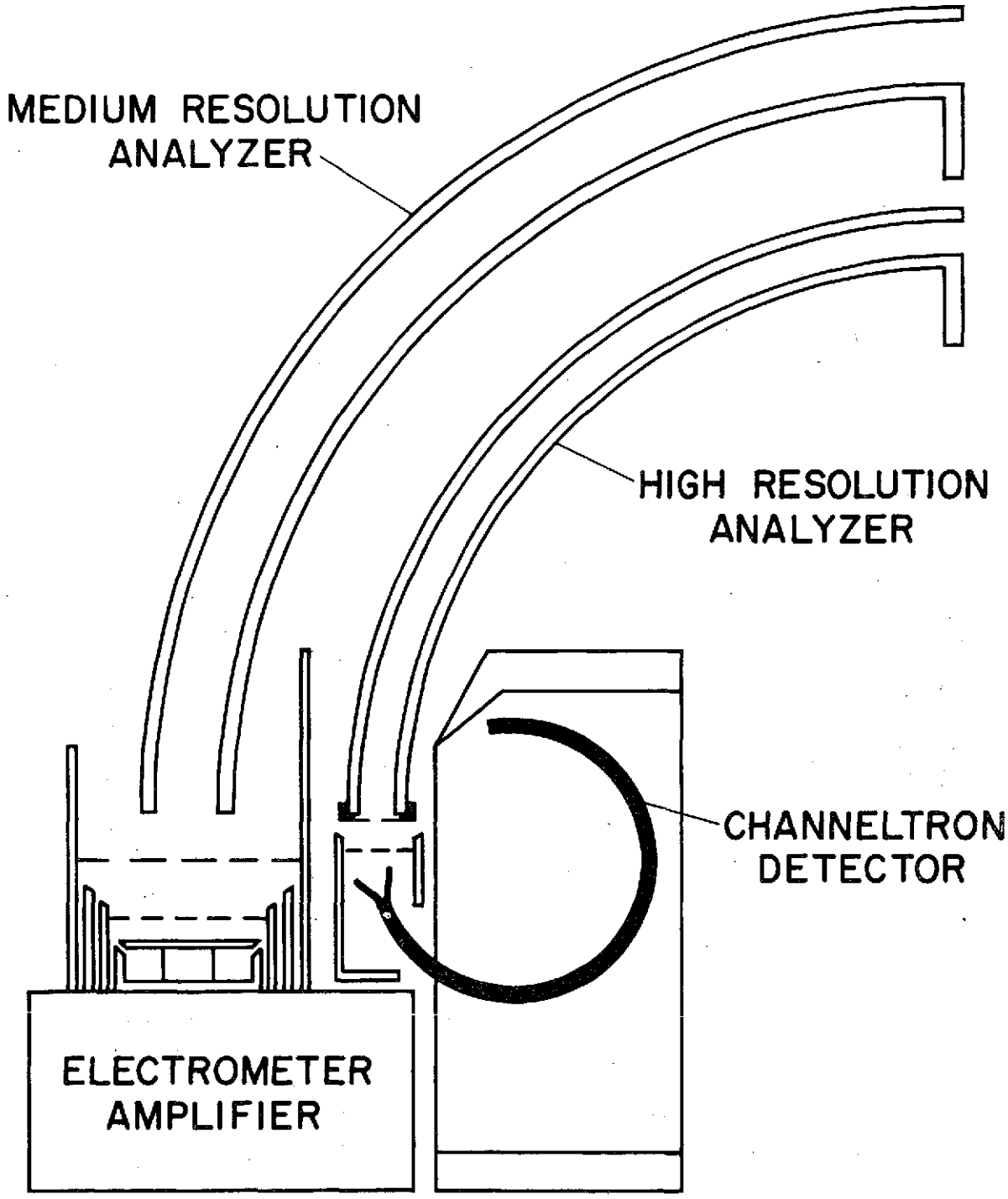
MEDIUM RESOLUTION
ANALYZER
HIGH RESOLUTION
ANALYZER
CHANNELTRON
DETECTOR
ELECTROMETER
AMPLIFIER

Figure 1

Figure 2

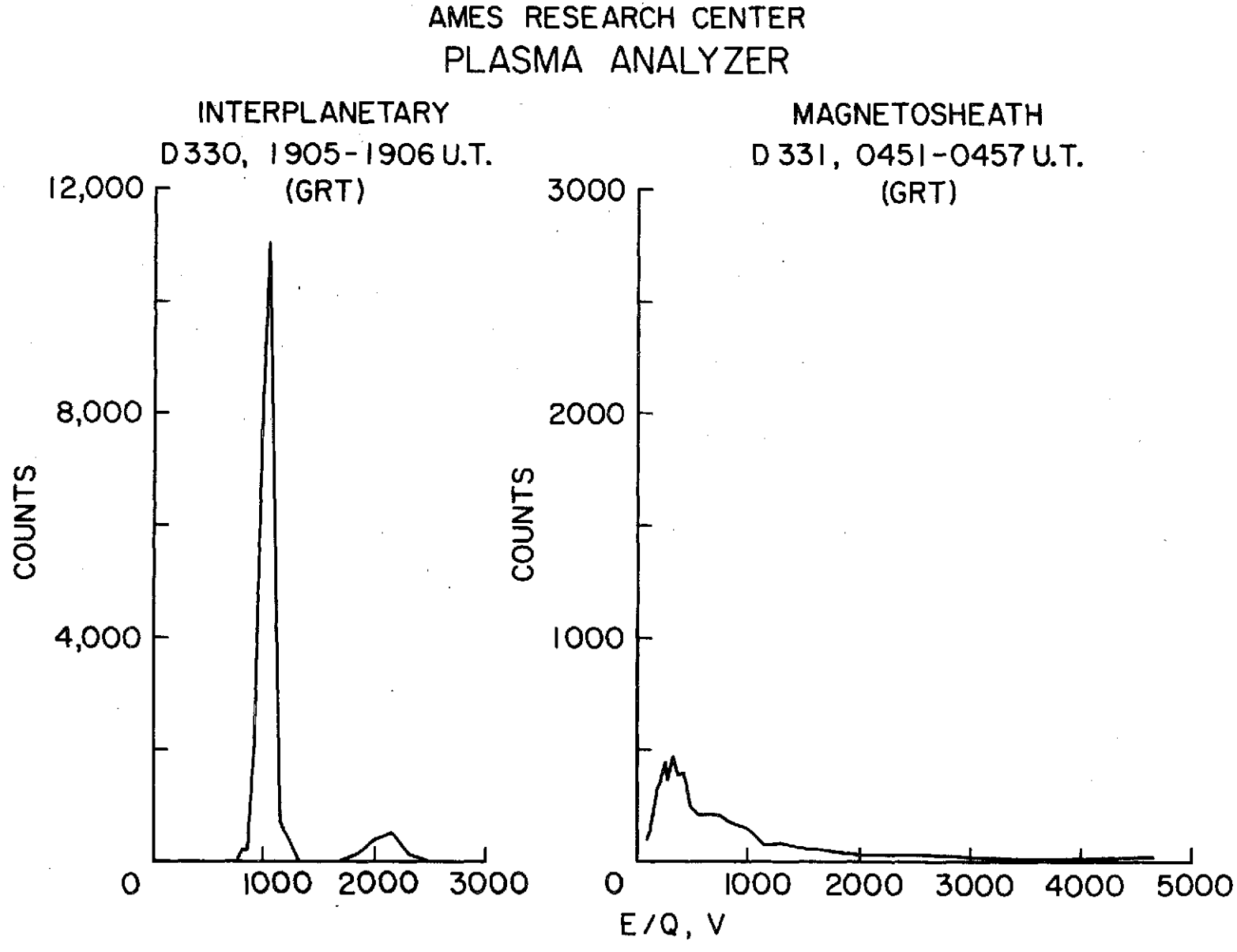
AMES RESEARCH CENTER
PLASMA ANALYZER
INTERPLANETARY
D330, 1905-1906 U.T.
(GRT)
12,000
8,000
4,000
0
COUNTS
1000
2000
3000
MAGNETOSHEATH
D331, 0451-0457 U.T.
(GRT)
3000
2000
1000
0
COUNTS
1000
2000
3000
4000
5000
E/Q, V

PIONEER 10-EXTREMES OF POSITION OF JUPITER'S MAGNETOPAUSE AND BOW SHOCK

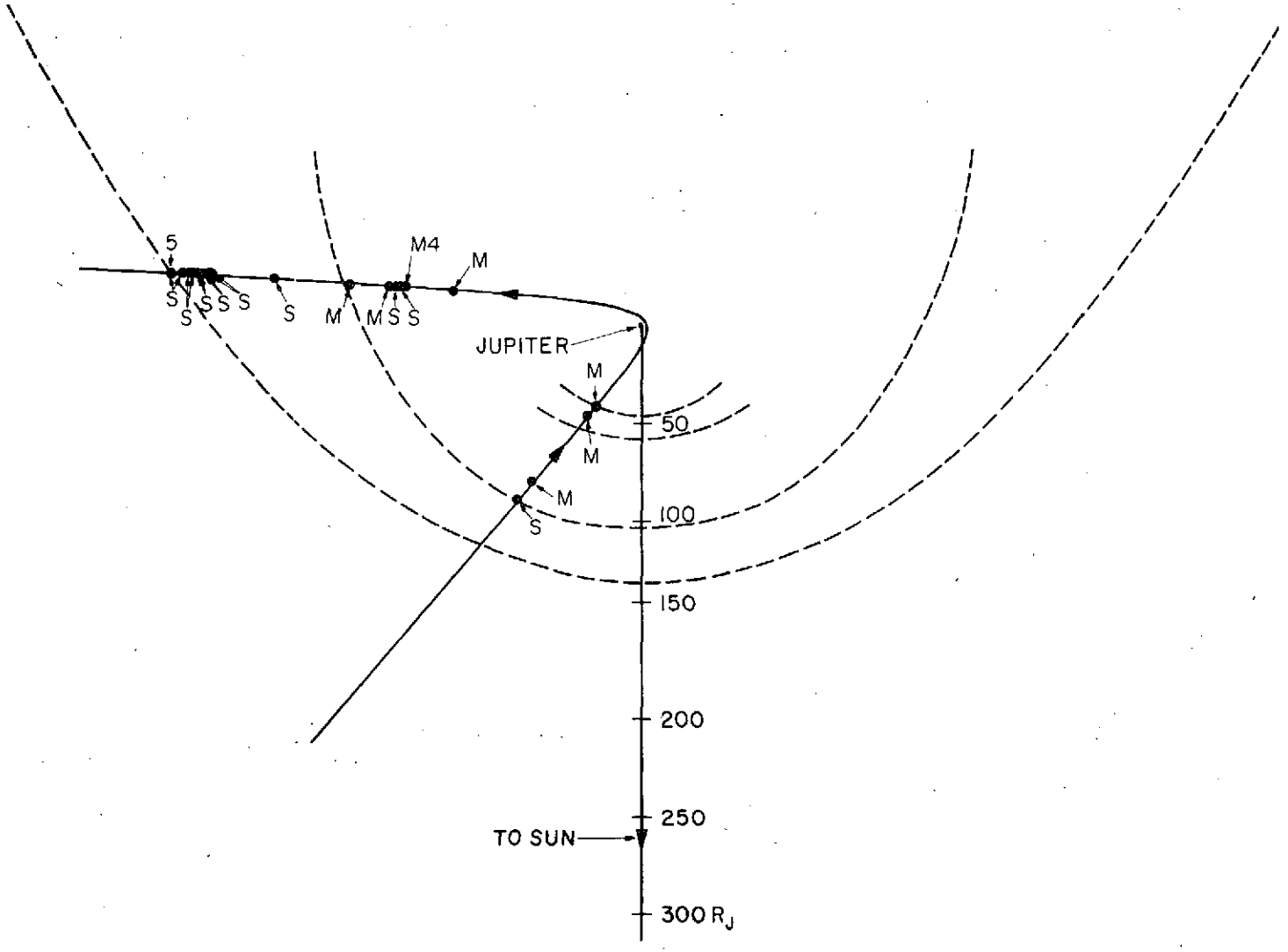

Figure 3

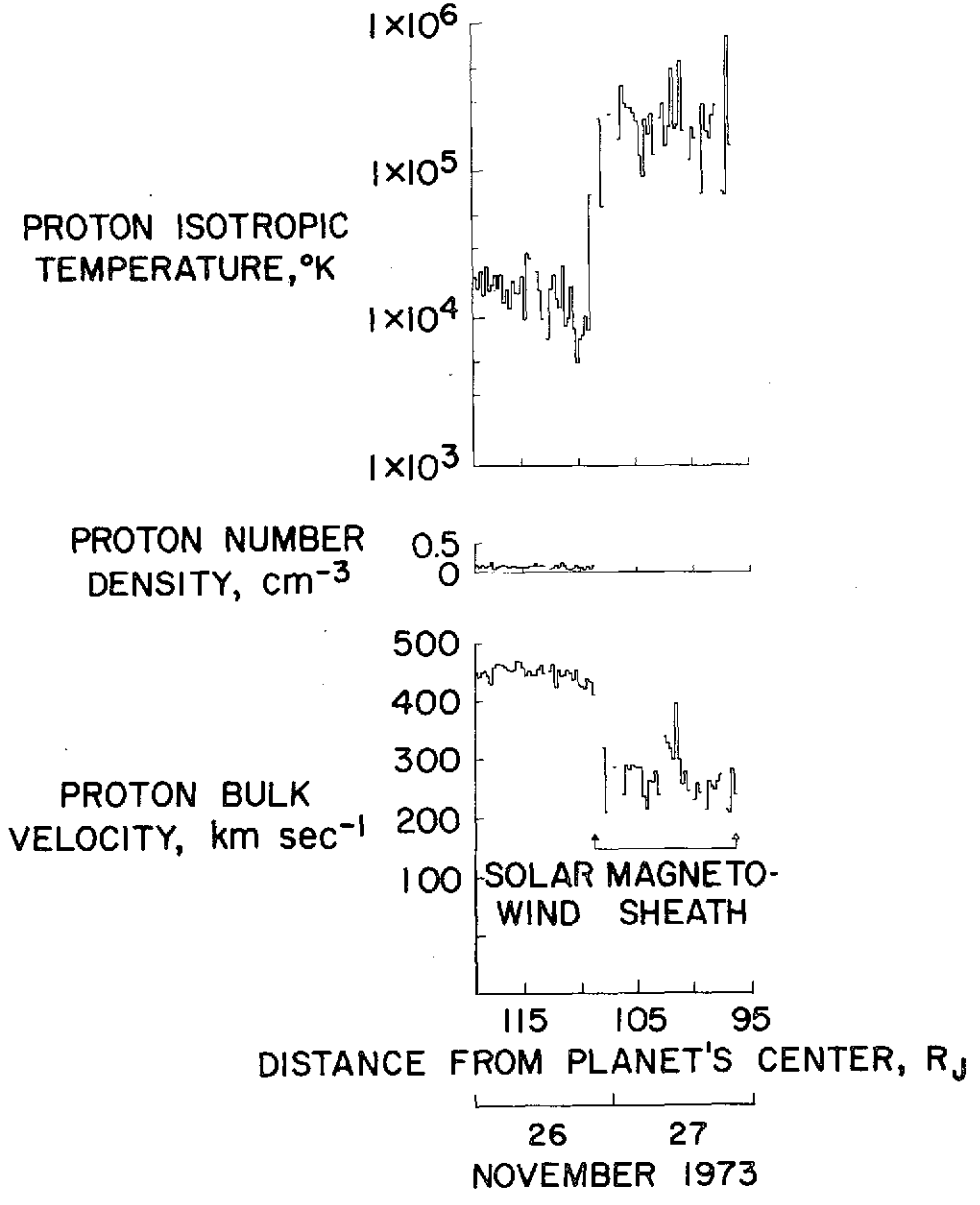
1×10^6
1×10^5
PROTON ISOTROPIC TEMPERATURE, °K
1×10^4
1×10^3
PROTON NUMBER DENSITY, cm^-3
0.5
0
500
400
300
PROTON BULK VELOCITY, km sec^-1
200
100
SOLAR MAGNETO-SHEATH
WIND
115
105
95
DISTANCE FROM PLANET'S CENTER, R_J
26
27
NOVEMBER 1973

Figure 4

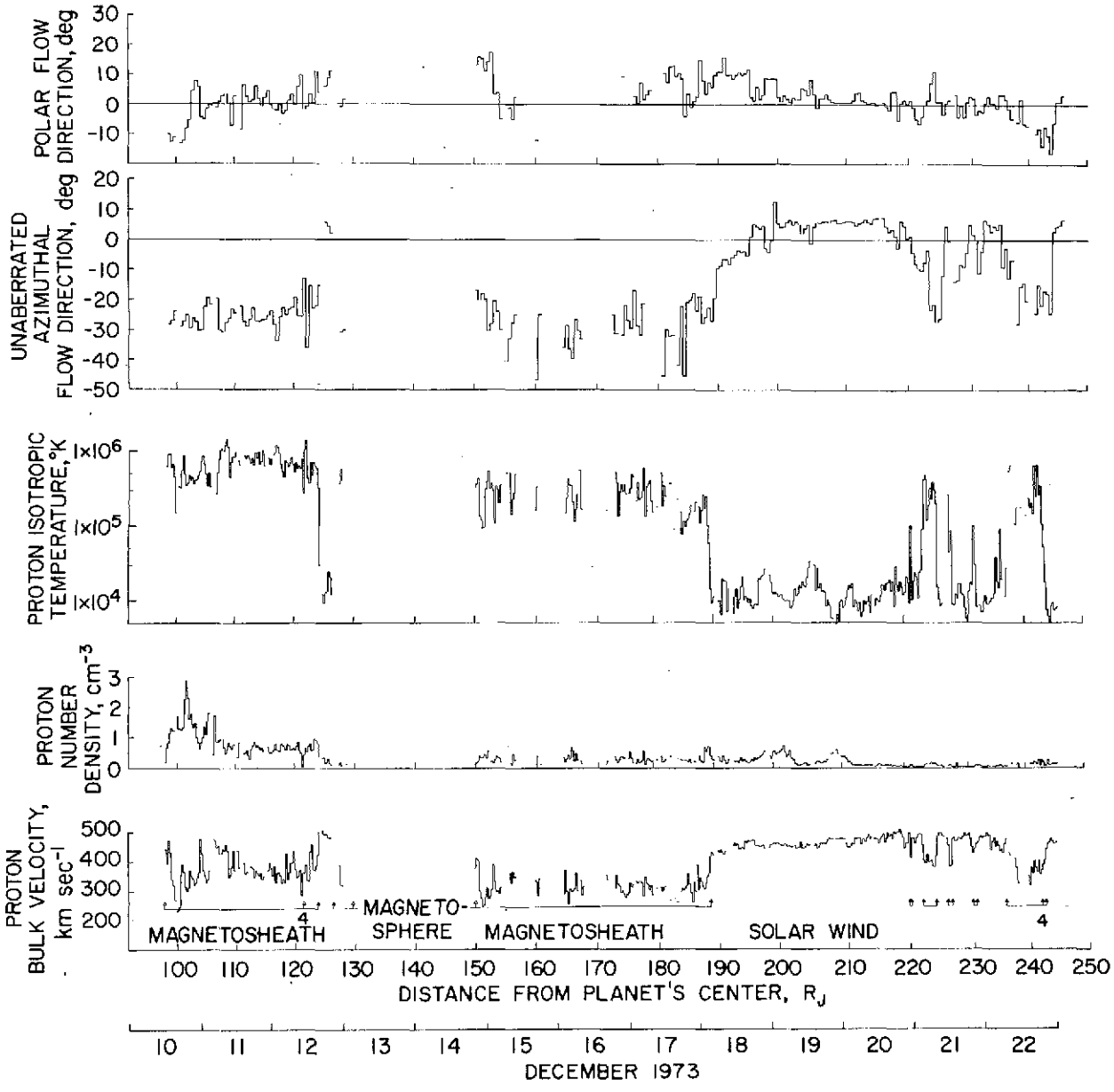
POLAR FLOW DIRECTION, deg
30
20
10
0
-10
UNABERRATED AZIMUTHAL FLOW DIRECTION, deg
20
10
0
-10
-20
-30
-40
-50
PROTON ISOTROPIC TEMPERATURE, °K
1×10^6
1×10^5
1×10^4
PROTON NUMBER DENSITY, cm^-3
3
2
1
0
PROTON BULK VELOCITY, km sec^-1
500
400
300
200
4
MAGNETOSHEATH
MAGNETO-SPHERE
MAGNETOSHEATH
SOLAR WIND
4
100 110 120 130 140 150 160 170 180 190 200 210 220 230 240 250
DISTANCE FROM PLANET'S CENTER, R_J
10 11 12 13 14 15 16 17 18 19 20 21 22
DECEMBER 1973

Figure 5